Sub-Picomolar Inhibition of HIV-1 Protease with a Boronic Acid

Ian W. Windsor,[†,‡] Michael J. Palte,[§,#] John C. Lukesh, III,[⊥] Brian Gold,[‡] Katrina T. Forest,*[,⊥,∥] and Ronald T. Raines*[,†,⊥,‡]

[†]Department of Biochemistry, [§]Medical Scientist Training Program, [#]Molecular & Cellular Pharmacology Graduate Training Program, [⊥]Department of Chemistry, and [∥]Department of Bacteriology, University of Wisconsin–Madison, Madison, Wisconsin 53706, United States; and [‡]Department of Chemistry, Massachusetts Institute of Technology, Cambridge, Massachusetts 02139, United States

*For K.T.F., E-mail: forest@bact.wisc.edu. Tel: 608-265-3566
*For R.T.R., E-mail: rtraines@mit.edu. Tel: 617-253-1470

Content	Page

General Experimental

Commercial reagents were used without further purification. (2*S*,3*S*)-1,2-epoxy-3-(Boc-amino)-4-phenylbutane was from Sigma–Aldrich (St. Louis, MO). All glassware was oven- or flame-dried, and reactions were performed under N_2(g) unless stated otherwise. Dichloromethane was dried over a column of alumina. Triethylamine was dried over a column of alumina and purified further by passage through an isocyanate scrubbing column. Flash chromatography was performed with columns of 40–63 Å silica, 230–400 mesh (Silicycle, Québec City, Canada). Thin-layer chromatography (TLC) was performed on plates of EMD 250-µm silica 60-F_{254}.

The term "concentrated under reduced pressure" refers to the removal of solvents and other volatile materials using a rotary evaporator at water aspirator pressure (<20 torr) while maintaining the water-bath temperature below 40 °C. Residual solvent was removed from samples at high vacuum (<0.1 torr). The term "high vacuum" refers to vacuum achieved by a mechanical belt-drive oil pump.

NMR spectra were acquired with a Bruker DMX-400 Avance spectrometer at the National Magnetic Resonance Facility at Madison (NMRFAM) and referenced to TMS or residual protic solvent. Electrospray ionization (ESI) mass spectrometry was performed with a Micromass LCT at the Mass Spectrometry Facility in the Department of Chemistry at the University of Wisconsin–Madison.

All procedures were performed in air at ambient temperature (~22 °C) and pressure (1.0 atm) unless indicated otherwise.

Chemical Synthesis

Scheme S1. Route for the synthesis of boronic acid **1.** Overall yield: 54% (unoptimized).

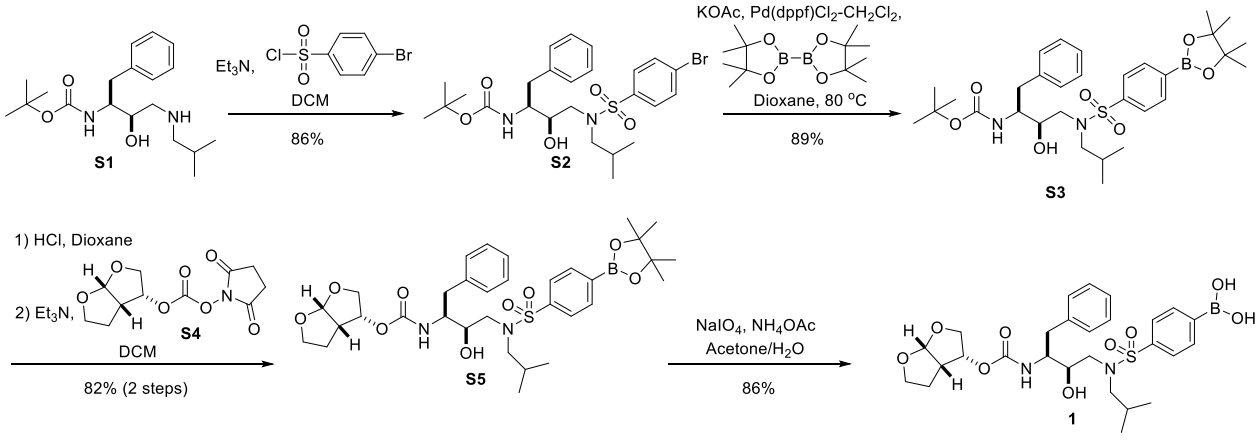

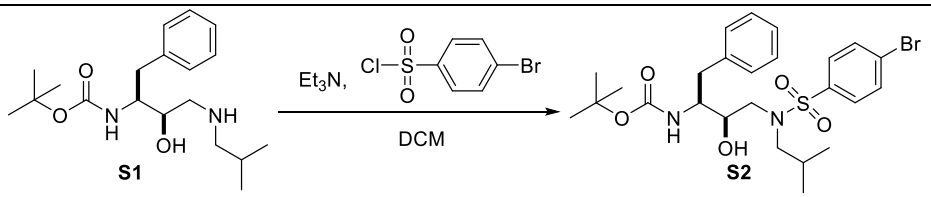

A round-bottom flask containing compound **S1** (1.791 g, 5.323 mmol; synthesized as described previously[1]) was dissolved in 60 mL of dichloromethane, and the resulting solution was cooled to 0 °C. Triethylamine (1.2 mL, 8.6 mmol) and 4-bromobenzenesulfonyl chloride (1.362 g, 5.330 mmol) were then added, and the reaction mixture was left to stir overnight under an atmosphere of dry N_2(g). After 16 h, the reaction mixture was concentrated under reduced pressure, and the product was purified by column chromatography (silica, 30% v/v EtOAc in hexanes), resulting in compound **S2** as a white solid (2.543 g, 86%). **^{1}H NMR** (400 MHz, $CDCl_3$, δ): 7.67–7.62 (m, 4H), 7.33–7.22 (m, 5H), 4.64 (d, J = 8.4 Hz, 1H), 3.87–3.76 (m, 3H), 3.11 (d, J = 6.1 Hz, 1H), 3.03–2.84 (m, 4H), 1.91–1.81 (m, 1H), 1.36 (s, 9H), 0.91 (d, J = 6.6 Hz, 3H), 0.88 (d, J = 6.6Hz, 3H). **^{13}C NMR** (100 MHz, $CDCl_3$, δ): 156.2, 137.8, 137.7, 132.5, 129.6, 128.9, 128.6, 127.9, 126.6, 79.9, 72.7, 58.4, 54.9, 53.4, 35.6, 28.4, 27.2, 20.2, 20.0. **HRMS–ESI** (m/z): $[M + Na]^+$ calcd for $C_{25}H_{35}BrN_2O_5SNa$, 577.1343; found, 577.1364.

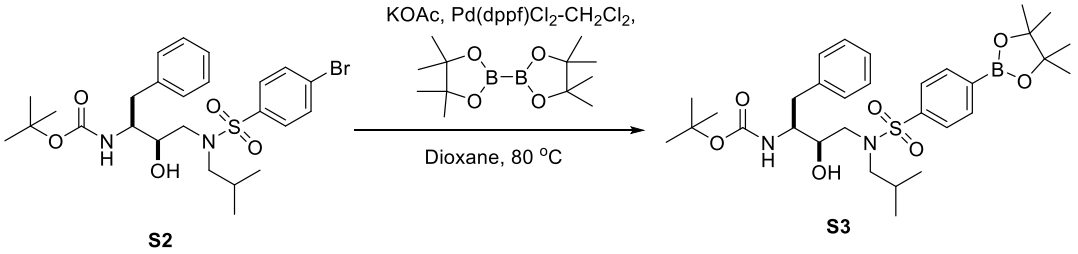

Compound **S2** (0.262 g, 0.472 mmol), KOAc (0.139 g, 1.416 mmol), bis(pinacolato)diboron (0.708 g, 2.78 mmol), and Pd(dppf)Cl_2–CH_2Cl_2 (34.54 mg, 0.0472 mmol) were placed in a dry Schlenk tube. The reaction flask was then evacuated and backfilled with N_2(g) five times. Freshly degassed 1,4-dioxane (5 mL) was then added, and the reaction mixture was heated to 80 °C and stirred for 24 h under a N_2(g) atmosphere. After 24 h, the reaction was vacuum filtered through a pad of Celite and concentrated under reduced pressure, and the product was purified by column chromatography (silica, 30% v/v EtOAc in hexanes), giving compound **S3** as a white solid (0.253 g, 89%). **^{1}H NMR** (400 MHz, $CDCl_3$, δ): 7.94 (d, J = 8.2 Hz, 2H), 7.75 (d, J = 8.2 Hz, 2H), 7.31–7.28 (m, 2H), 7.25–7.21 (m, 3H), 4.67 (d, J = 8.6 Hz, 1H), 3.93–3.91 (m, 1H), 3.84–3.81 (m, 1H), 3.78–3.74 (m, 1H), 3.13–3.06 (m, 2H), 3.01–2.81 (m, 4H), 1.89–1.81 (m, 1H), 1.36 (s, 12H), 1.35 (s, 9H), 0.89 (d, J = 6.6 Hz, 3H), 0.86 (d, J = 6.6 Hz, 3H). **^{13}C NMR** (100 MHz, $CDCl_3$, δ): 156.1, 140.6, 137.9, 135.5, 129.7, 128.6, 126.5, 126.4, 84.6, 79.8, 72.8, 58.6, 54.9, 53.7, 35.5, 29.8, 28.4, 27.2, 25.0, 20.2, 20.0. **HRMS–ESI** (m/z): $[M + Na]^+$ calcd for $C_{31}H_{47}BN_2O_7SNa$, 624.3126; found, 624.3151.

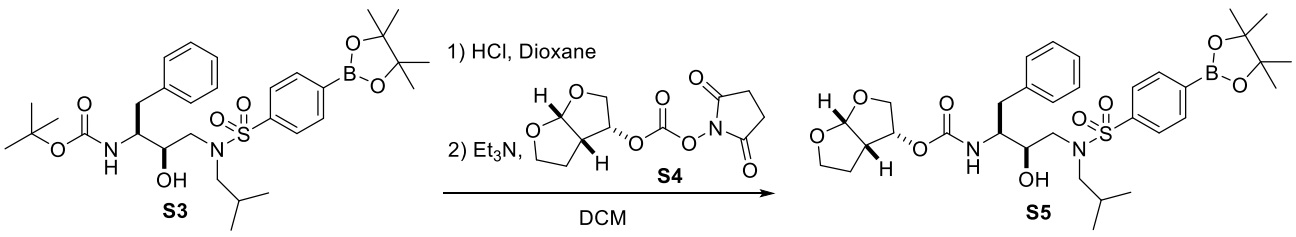

To a round-bottom flask containing compouind **S3** (0.327 g, 0.543 mmol) was added 15 mL of 4.0 M HCl in dioxane. After stirring for 4 h, the reaction mixture was purged with N_2(g) to remove excess HCl(g). Once the evolution of HCl(g) ceased, the reaction mixture was concentrated under reduced pressure and dried overnight under high vacuum. The residue was then dissolved in 10 mL of DCM and placed under an inert atmosphere. Triethylamine (0.38 mL, 2.7 mmol) and compound **S4** (0.147 g, 0.543 mmol; synthesized as described previously[1]) were then added, and the reaction mixture was stirred overnight. After reacting for 16 h, the reaction was concentrated under reduced pressure, and the product was purified by column chromatography (silica, 5% v/v MeOH in DCM), yielding compound **S5** as a white solid (0.293 g, 82%). **^{1}H NMR** (400 MHz, $CDCl_3$, δ): 7.94 (d, J = 7.6 Hz, 2H), 7.75 (d, J = 7.6 Hz, 2H), 7.30–7.26 (m, 2H), 7.22–7.20 (m, 3H), 5.65 (d, J = 5.1 Hz, 1H), 5.04–4.99 (m, 1H), 4.95–4.92 (m, 1H), 3.96 (t, J = 8.2 Hz, 1H), 3.88–3.83 (m, 3H), 3.72–3.68 (m, 2H), 3.63–3.59 (m, 1H), 3.20–3.14 (m, 1H), 3.09–3.05 (m, 1H), 3.02–2.97 (m, 2H), 2.93–2.87 (m, 1H), 2.83–2.78 (m, 2H), 1.87–1.79 (m, 1H), 1.49–1.43 (m, 1H), 1.36 (s, 12H), 1.26–1.24 (m, 1H), 0.93 (d, J = 6.5 Hz, 3H), 0.87 (d, J = 6.5 Hz, 3H). **^{13}C NMR** (100 MHz, $CDCl_3$, δ): 155.4, 140.1, 137.5, 135.4, 129.3, 128.6, 126.6, 126.3, 109.3, 84.5, 73.4, 72.7, 70.7, 69.6, 58.0, 55.1, 53.7, 45.3, 35.6, 27.3, 25.8, 24.9, 24.8, 20.1, 19.8; **HRMS–ESI** (m/z): $[M + NH_4]^+$ calcd for $C_{33}H_{51}BN_3O_9S$, 676.3431; found, 676.3440.

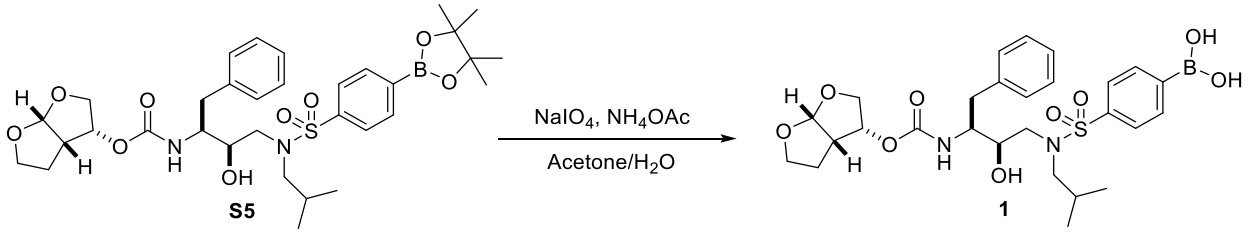

A round-bottom flask was charged with compound **S5** (0.150 g, 0.228 mmol), which was dissolved in acetone (10 mL) and H_2O (10 mL). The resulting solution was placed under an atmosphere of dry N_2(g), and sodium periodate (0.195 g, 0.911 mmol) and ammonium acetate (70.2 mg, 0.911 mmol) were added. After stirring for 12 h, the reaction mixture was concentrated under reduced pressure, and the product was purified by column chromatography (silica, 20% v/v MeOH in DCM), giving rise to compound **1** as an off-white solid (0.113 g, 86%). An analytically pure sample of compound **1** was obtained by reverse-phase HPLC using a preparatory C18 column and a linear gradient of 10–80% v/v acetonitrile (0.1% v/v TFA) in water (0.1% v/v TFA) over 45 min. Compound **1** eluted at 38 min and, after lyophilization, was isolated as a white powder. **^{1}H NMR** (400 MHz, methanol-d_4, δ): 7.81 (s, 4H), 7.26–7.21 (m, 4H), 7.20–7.15 (m, 1H), 5.59 (d, J = 5.0 Hz, 1H), 4.93 (q, J = 6.4 Hz, 1H), 3.93 (dd, J = 9.9, 6.2 Hz, 1H), 3.84–3.65 (m, 5H), 3.46–3.43 (m, 1H), 3.21–3.10 (m, 2H), 2.99–2.84 (m, 3H), 2.53 (dd, J = 14.3, 10.4 Hz, 1H), 2.07–1.99 (m, 1H), 1.54–1.46 (m, 1H), 1.37–1.32 (m, 1H), 0.94 (d, J = 6.6 Hz, 3H), 0.88 (d, J = 6.6 Hz, 3H). **^{13}C NMR** (100 MHz, methanol-d_4, δ): 157.7, 140.3, 135.2, 135.1, 130.5, 129.3, 127.4, 127.2, 110.8, 74.6, 74.5, 72.1, 70.6, 58.9, 57.4, 53.9, 46.9, 37.2, 28.0, 27.0, 20.5, 20.4. **HRMS–ESI** (m/z): $[M + OMe]^-$ calculated for $C_{30}H_{44}BN_2O_{10}S$, 635.2814; found, 635.2821.

Protein Preparation

Wild-type HIV-1 protease and its D30N variant were produced heterologously in *Escherichia coli* and purified as described previously.[2] This HIV-1 protease had Q7K, L33I, L63I, C67A, and C95A substitutions. Protease solutions in 1 mM sodium acetate buffer, pH 5.0, containing NaCl (2 mM) were concentrated to 4.0 mg/mL (wild-type) or 15 mg/mL (D30N), flash-frozen in N_2(l), and stored at –80 °C. The flash-freezing was done within 30 min of elution from the gel-filtration column. On the day of an assay, a concentrated stock solution was thawed rapidly, incubated on ice and diluted with room-temperature assay buffer (50 mM sodium acetate buffer, pH 5.0, containing 0.10 M NaCl) to create a 20× stock solution, which was then used immediately for assays.

Enzyme Kinetics

Instrumentation and Materials

Assays for the catalytic activity of wild-type HIV-1 protease and its D30N variant were conducted with a fluorogenic substrate, RE(Edans)SGIFLETSK(Dabcyl)R, and an M1000 plate reader (Tecan) as described previously.[2a] In these assays, all reactions were initiated nearly simultaneously, that is, within a few seconds. All linear and non-linear regression analyses were performed with Prism 6 software from GraphPad (La Jolla, CA).

Michaelis–Menten Kinetics

Michaelis–Menten kinetics were performed to assess the impact of the D30N substitution on the catalytic activity of HIV-1 protease. As observed previously,[3] the D30N substitution decreases the value of k_{cat} by about an order of magnitude, from 7.4 s^{-1} to 0.50 s^{-1}, and increases the value of K_M slightly, from 15 μM to 16 μM.[2a] These values were used as parameters in the fitting of data acquired in the presence of inhibitors. Reaction progress curves were fitted by linear regression to determine reaction velocities (Figure S1A). Non-linear regression analyses of the resulting data were performed with the mean reaction velocity, its standard deviation, and the number of reactions per data point (n) (Figure S1B). Reactions were performed in quadruplicate (n = 4).

Inhibition Kinetics

The Morrison equation[4] was used to evaluate values of K_i that were lower than the concentration of enzyme used in assays, essentially as described previously.[2a] In these assays, the initial fluorescence of assay buffer containing substrate and inhibitor in a combined volume of 190 μL was measured. Measurement was paused briefly for the addition of the 20× stock solution of enzyme. Data collected immediately after the addition of enzyme and prior to achieving enzyme–inhibitor equilibrium were omitted from the analyzed data set. The mean velocity and its standard deviation (derived from linear regression) at a particular concentration of inhibitor were normalized to the velocity in the absence of inhibitor. These normalized values were fitted with the "Morrison Ki" subroutine in Prism 6 software. The Morrison equation can be used to determine the enzyme concentration, but doing so led to wild-type enzyme concentrations that differed by

>20% from concentrations measured by active-site titration with darunavir. Accordingly, wild-type enzyme concentrations were set to the value derived from the Michaelis–Menten equation in the absence of inhibitor, as described previously.[2a] These values agreed well (<10% variation) with those measured by active-site titration. In contrast, the D30N enzyme concentrations provided by the Morrison equation agreed well (<10% variation) with those measured by active-site titration with darunavir. Accordingly, D30N enzyme concentrations were fitted simultaneously with values of K_i by using the "Morrison Ki" subroutine in Prism 6 software.

Cytotoxicity

MT-4 cells (catalog #120) and darunavir (catalog #11447) were obtained from the AIDS Reagent Program of the NIAID (NIH). Cells were grown at 37 °C in RPMI 1640 containing fetal bovine serum (10% v/v) and Hyclone antibiotic/antimycotic solution (1% v/v) from GE Healthcare (Chicago, IL). Cells were plated at a density of 2.5×10^4 cells per 100 µL in a flat-bottomed, 96-well plate from Corning (Corning, NY). Concentrated protease inhibitor stocks were prepared at 200 mM in DMF and diluted by ≥200-fold with final a solvent content of 0.5% by volume in each condition. After incubation at 37 °C for 48 h, cells were assayed for viability using the CellTiter 96® AQ_{ueous} One Solution Cell Proliferation MTS Assay from Promega (Madison, WI) by monitoring absorbance at 450 nm with a GloMax multidetection plate reader from Promega. Each condition was assayed in triplicate.

X-Ray Crystallography

Protein Crystallization

Compound **1** was dissolved in DMF at a concentration of 15 mg/mL. Hanging drop vapor-diffusion plates were setup by mixing a protease stock solution with the ligand stock solution at ratios of 1:9 (wild-type:**1**) or 1:4 (D30N:**1**) in 2-µL drops over a reservoir of 100 mM Tris–HCl buffer, pH 7.4, containing NaCl (200 mM for wild-type; 400 mM for D30N). Crystals grew within 2–3 days. Crystals were cryo-protected in mother liquor containing 25% v/v glycerol and flash-frozen in N_2(l).

X-Ray Diffraction

Diffraction experiments were conducted at the Advanced Photon Source of Argonne National Lab with the Life Sciences Collaborative Access Team at sector 21. Frames were indexed, integrated, and scaled with HKL2000 (HKL Research). Details of the diffraction experiment are listed in Table S1.

Structure Solution and Refinement

Molecular replacement (MR) was conducted using Phaser software as implemented in Phenix using 3nu3 as a reference model with solvent, ligand, and alterative conformations removed.[5] The MR solution was refined with Phenix Refine, and further model building was conducted with Coot.[6] The atomic coordinates of boronic acid **1** in an idealized conformation were prepared using

WebMO (WebMO, LLC). The final geometry was optimized by the AM1 method and restraints were prepared with eLBOW in Phenix. Compound **1** bound to the wild-type protease in two antiparallel conformations with unequal occupancy (Figure S2A). The boronic acid was only well resolved in the major conformation with 0.7 occupancy. Two conformations of Asp30 were also resolved with major and minor conformers. The conformers of the ligand and Asp30 that had similar occupancies are believed to be the pair that participate in a hydrogen bond (Figures 1G and S2A). There was sufficient density only in the lower-resolution structure of the D30N protease complex to place a single molecule of boronic acid **1** and determine the conformation of Asn30 (Figure S2B). The major conformers in the wild-type structure are nearly identical to the single conformation in the structure of the D30N protease complex (Figures 2G and 2H). Details of the final refined structures are listed in Table S1.

Computational Analysis

DFT optimization with Gaussian

Simplified models of the low-barrier hydrogen bonding (LBHB) interactions were extracted from the X-ray structures of compound **1** bound to wild-type HIV-1 protease and its D30N variant. Average coordinate errors for the structures can be found in Table 1. The ligand was truncated after the sulfonamide, leaving behind two methyl groups on the nitrogen to maintain sterics. The entire Asp30 or Asn30 residue along with flanking main-chain amide bonds with the distal C^{α} as a methyl group were included. DFT calculations were used to optimize hydrogens with Gaussian 16, Revision A.03 software from Gaussian (Wallingford, CT).[7] Proton optimization was conducted at the M06-2X/6-311+G(d,p) level of theory employing the IEFPCM solvation model.

Natural Bonding Orbital Analysis

NBO analysis was conducted with NBO 6.0 software,[8] using the $CHOOSE keyword to give the Lewis structure where the boronic acid acts as the proton donor (the proton is bonded to the boronic acid oxygen). When the $CHOOSE keyword is not utilized, the NBO program generates a low valence proton sandwiched between two oxyanions. NBO analysis shows the dominant interaction is with the in-plane, predominantly *p*-type lone pair of the carboxylate oxygen. The strength of the LBHB interaction is likely largely overestimated at 69.8 kcal/mol (taken as the 2nd-order perturbation energy minus the steric exchange). The D30N substitution weakens the interaction to 58.3 kcal/mol. To model attenuation of the carboxylate charge via external H-bonding, the strength of the interaction with the acid was investigated and found to be 40.7 kcal/mol. The highly covalent nature of this hydrogen bond is apparent. In addition to large interaction energies, hybridization of the carboxylate lone pair from *p* to $sp^{3.99}$ ($sp^{3.93}$ for the D30N amide) is observed in the NBO analysis. Lone pairs involved in hydrogen bonding on each oxygen hybridize when $CHOOSE is not used.

Atoms in Molecules (AIM) Analysis

To investigate further the covalency of the SSHB, we turned to an alternative description of chemical bonding—the bond critical point (BCP) concept stemming from the topological quantum theory of atoms in molecules (AIM) developed Bader.[9] Here, structural elements are identified by critical points of electron density ($\nabla\rho = 0$), with atoms at maxima and bonds at minima. The sign of the Laplacian ($\nabla^2\rho$) at the BCP gives insights into bonding character, with covalent bonds showing a negative value and ionic bonds positive. Previous investigations have found that LBHB have a substantial degree of covalency and in extreme cases can exist as a 2-center, 3-center bond.[10]

AIMAll (Version 17.01.25) was used for atoms in molecules (AIM) calculations (Table S2). We found a covalent character between the proton and both oxygens, with a calculated electron density of 0.270 eÅ^{-3} and 0.174 eÅ^{-3} at the BCP for the BO–H and BOH···OC bonds, respectively. Additionally, the $\nabla^2\rho$ was negative for both bonds at –1.38 eÅ^{-5} and –0.08 eÅ^{-5}, respectively. Bond indices were 0.31 and 0.22, respectively. Typical O···H hydrogen bonds display bond orders <0.1, $\rho < 0.2$ eÅ^{-3}, and positive Laplacian values.[10b] Thus, we report a short, asymmetric hydrogen bond with substantial covalent character. The bond in the D30N variant gives similar values, although the covalency is slightly diminished.

Hydrogen Optimization Coordinates

```
Wild-Type HIV-1 Protease H-opt
 C               2.25266200   -0.62212600    3.27668600
 C               3.23915400    0.11419000    2.38597100
 O               4.33882100    0.48036300    2.81953200
 N               2.87914700    0.28897600    1.11728800
 C               3.78769100    0.84787400    0.13252900
 C               3.19569700    2.10728300   -0.47630900
 O               2.00652700    2.40464800   -0.33961800
 C               4.10431100   -0.15093900   -0.98900400
 C               4.37662400   -1.55330000   -0.47286100
 O               3.55684600   -2.45545100   -0.75590400
 O               5.41560800   -1.75013600    0.19012900
 N               4.06440200    2.84452000   -1.14662100
 C               3.72329800    4.07932400   -1.83190400
 C              -5.14279700   -0.39997100    2.03323800
 N              -5.24254700    0.73572600    1.16671100
 S              -5.01267200    0.48412600   -0.45353900
 C              -4.93421600    1.98868900    1.76162400
 O              -4.99906600    1.73728200   -1.10641600
 O              -5.93429700   -0.49749600   -0.87425200
 O               0.55958400   -3.61106600   -0.94613300
 O               1.56085700   -1.51851600   -0.86930700
 C              -3.40535400   -0.20819400   -0.62101900
 C              -3.24347700   -1.58515100   -0.69608700
 C              -2.03415200   -2.19963700   -0.79049300
 C              -0.85659700   -1.49815900   -0.80740500
 C              -0.95695400   -0.07589400   -0.71027600
 C              -2.20639000    0.52101800   -0.62403800
 B               0.46016100   -2.25397700   -0.89947000
 H               2.08207200   -0.03053600    4.17608400
 H               1.30196800   -0.81852900    2.78152200
 H               2.70856100   -1.56772500    3.57372600
 H               4.70272900    1.09645200    0.67047500
 H               3.28281000   -0.16649500   -1.70546900
 H               5.00296100    0.18313600   -1.51185000
 H               5.02931000    2.55003800   -1.16676900
 H               3.37539600    4.83147300   -1.12171300
 H               4.61038100    4.44901800   -2.33967400
 H               2.93628400    3.90230900   -2.56616700
 H              -5.77261400   -0.22908800    2.90786100
 H              -5.50228500   -1.29879500    1.53235500
 H              -4.11114200   -0.56542800    2.37006600
 H              -5.61718600    2.15259100    2.59798500
 H              -5.07506100    2.79726600    1.04742700
 H              -3.90555900    2.02556000    2.14457500
 H               1.47651200   -3.90241200   -0.94910500
 H               2.47420200   -2.00591500   -0.94438700
 H              -4.13898700   -2.20073300   -0.69582600
 H              -2.00887000   -3.28264000   -0.85591300
 H              -0.06258900    0.53756800   -0.71249800
 H              -2.25705000    1.60540500   -0.56682100
 H               2.02704500   -0.13026100    0.75827100
HF: -1774.6501795
```

D30N HIV-1 Protease H-opt

C	2.13045000	-0.68338500	3.26827500
C	3.12292300	0.07919400	2.39279800
O	4.23756100	0.39997000	2.82903600
N	2.73815100	0.35702900	1.14819400
C	3.62784200	0.88726600	0.12987600
C	3.06809700	2.18504100	-0.43967400
O	1.87279600	2.46825100	-0.36044000
C	3.81578800	-0.11316000	-1.02318200
C	4.40488700	-1.43411700	-0.57497500
N	5.65215500	-1.40038800	-0.10038800
O	3.75114300	-2.48334800	-0.67465300
N	3.96108100	2.95740800	-1.04330800
C	3.60732200	4.20749400	-1.70527900
C	-5.16375400	-0.46833700	2.01660800
N	-5.33696700	0.67369000	1.14702600
S	-5.05922900	0.46809100	-0.50353500
C	-5.09386600	1.89730900	1.76276900
O	-5.04022900	1.74737400	-1.13490700
O	-5.99062400	-0.45708700	-1.03186700
O	1.83380700	-1.59797000	-0.87131800
O	0.67580300	-3.63479900	-0.88195700
C	-3.39102100	-0.25143900	-0.61264200
C	-2.19298300	0.48039300	-0.49372600
C	-0.91487300	-0.12499600	-0.56782000
C	-0.74862100	-1.52913700	-0.73696700
C	-1.94851600	-2.24427900	-0.83438900
C	-3.18640100	-1.63261600	-0.77080900
B	0.64644500	-2.26006400	-0.82806100
H	4.57478800	0.32773700	-1.68218000
H	2.91811500	-0.22740300	-1.60345000
H	6.17615000	-0.54069300	-0.05189000
H	6.09355600	-2.25255100	0.21494200
H	4.57811100	1.08958300	0.62719500
H	1.16657500	-0.83388000	2.78278400
H	1.87677500	-0.04808900	0.80440900
H	2.57210600	-1.65124200	3.50874100
H	1.99280800	-0.13011300	4.19686600
H	4.93419900	2.69149800	-1.02315100
H	4.50093100	4.61505000	-2.17066600
H	2.85058400	4.02724100	-2.46940300
H	3.21443400	4.92568700	-0.98405600
H	-5.43906800	-1.38981800	1.50220700
H	-4.12879000	-0.54718800	2.37125900
H	-5.82713500	-0.34789800	2.87390400
H	-5.25551800	2.72504700	1.07350800
H	-4.07429700	1.97704500	2.16828500
H	-5.79401500	2.02211400	2.59327000
H	2.61656500	-2.23063300	-0.93202500
H	-0.17255900	-4.07452400	-0.80524400
H	-2.23509200	1.55864800	-0.36903200
H	-0.04674800	0.52472300	-0.49893700
H	-1.95850700	-3.31934100	-0.97807700
H	-4.06516600	-2.26481000	-0.86938500

HF: -1755.2029447

References

(1) Surleraux, D. L.; Tahri, A.; Verschueren, W. G.; Pille, G. M.; de Kock, H. A.; Jonckers, T. H.; Peeters, A.; De Meyer, S.; Azijn, H.; Pauwels, R.; de Bethune, M. P.; King, N. M.; Prabu-Jeyabalan, M.; Schiffer, C. A.; Wigerinck, P. B. *J. Med. Chem.* **2005**, *48*, 1813–1822.

(2) (a) Windsor, I. W.; Raines, R. T. *Sci. Rep.* **2015**, *5*, 11286. (b) Windsor, I. W.; Raines, R. T. *Acta Crystallogr.* **2018**, *D74*, 690–694.

(3) Kovalevsky, A. Y.; Tie, Y.; Liu, F.; Boross, P. I.; Wang, Y.-F.; Leshchenko, S.; Ghosh, A. K.; Harrison, R. W.; Weber, I. T. *J. Med. Chem.* **2006**, *49*, 1379–1387.

(4) (a) Williams, J. W.; Morrison, J. F. *Methods Enzymol.* **1979**, *63*, 437-467. (b) Greco, W. R.; Hakala, M. T. *J. Biol. Chem.* **1979**, *254*, 12104–12109. (c) Murphy, D. J. *Anal. Biochem.* **2004**, *327*, 61–67.

(5) Adams, P. D.; Afonine, P. V.; Bunkoczi, G.; Chen, V. B.; Davis, I. W.; Echols, N.; Headd, J. J.; Hung, L. W.; Kapral, G. J.; Grosse-Kunstleve, R. W.; McCoy, A. J.; Moriarty, N. W.; Oeffner, R.; Read, R. J.; Richardson, D. C.; Richardson, J. S.; Terwilliger, T. C.; Zwart, P. H. *Acta Crystallogr.* **2010**, *D66*, 213–221.

(6) Emsley, P.; Lohkamp, B.; Scott, W. G.; Cowtan, K. *Acta Crystallogr.* **2010**, *D66*, 486–501.

(7) Frisch, M. J.; Trucks, G. W.; Schlegel, H. B.; G. E. Scuseria; Robb, M. A.; Cheeseman, J. R.; Scalmani, G.; Barone, V.; Petersson, G. A.; Nakatsuji, H.; Li, X.; Caricato, M.; Marenich, A. V.; Bloino, J.; Janesko, B. G.; Gomperts, R.; Mennucci, B.; Hratchian, H. P.; Ortiz, J. V.; Izmaylov, A. F.; Sonnenberg, J. L.; D. Williams-Young; Ding, F.; Lipparini, F.; Egidi, F.; Goings, J.; Peng, B.; Petrone, A.; Henderson, T.; Ranasinghe, D.; Zakrzewski, V. G.; Gao, J.; Rega, N.; Zheng, G.; Liang, W.; Hada, M.; Ehara, M.; Toyota, K.; Fukuda, R.; Hasegawa, J.; Ishida, M.; Nakajima, T.; Honda, Y.; Kitao, O.; Nakai, H.; Vreven, T.; Throssell, K.; J. A. Montgomery, J.; Peralta, J. E.; Ogliaro, F.; Bearpark, M. J.; Heyd, J. J.; Brothers, E. N.; Kudin, K. N.; Staroverov, V. N.; Keith, T. A.; Kobayashi, R.; Normand, J.; Raghavachari, K.; Rendell, A. P.; Burant, J. C.; Iyengar, S. S.; Tomasi, J.; Cossi, M.; Millam, J. M.; Klene, M.; Adamo, C.; Cammi, R.; Ochterski, J. W.; Martin, R. L.; Morokuma, K.; Farkas, O.; Foresman, J. B.; Fox, D. J. *Gaussian 16, Revision A.03*. Gaussian, Inc.: Wallingford CT, 2016.

(8) E. D. Glendening, J., K. Badenhoop, A. E. Reed, J. E. Carpenter, J. A. Bohmann, C. M. Morales, C. R. Landis, and F. Weinhold *NBO 6.0*, Theoretical Chemistry Institute, University of Wisconsin: Madison, WI, 2013.

(9) Bader, R. F. W. *Chem. Rev.* **1991**, *91*, 893–928.

(10) (a) Schiott, B.; Iversen, B. B.; Madsen, G. K.; Larsen, F. K.; Bruice, T. C. *Proc. Natl. Acad. Sci. USA* **1998**, *95*, 12799–12802. (b) Molčanov, K.; Jelsch, C.; Wenger, E.; Stare, J.; Madsen, A. Ø.; Kojić-Prodić, B. *CrystEngComm* **2017**, *19*, 3898–3901.

Table S1. Crystallographic Data Collection and Refinement Statistics

Complex	**Wild-Type**	**D30N**
PDB code	6c8x	6c8y
Data Collection		
X-ray source	21-ID-D	21-ID-F
Detector	MAR 300 CCD	MAR 225 CCD
Wavelength, Å	0.97853	0.97872
Resolution Å (last shell)	27.0–1.60 (1.63–1.60)	48.8–1.94 (1.97–1.94)
Space group	P 2_12_12	P 2_12_12
a, b, c (Å)	58.7, 86.2, 46.2	59.1, 86.4, 45.8
α, β, γ (°)	90, 90, 90	90, 90, 90
No. of Reflections	437,309	128,391
No. Unique Reflections	30,670 (1507)	17,966 (874)
Redundancy (last shell)	14.3 (13.2)	7.1 (7.0)
Mean I/σ (last shell)	38.3 (3.5)	13.9 (2.7)
Completeness (last shell)	100 (100)	100 (100)
R_{meas} (last shell)	0.095 (0.667)	0.119 (0.671)
R_{sym}	0.092 (0.642)	0.111 (0.621)
R_{pim}	0.025 (0.181)	0.044 (0.250)
Wilson B-factor	15.5	21.7
Refinement		
Working set (last shell)	30,625 (2,779)	17,927 (1,760)
Test set (last shell)	1,508 (132)	877 (88)
R_{work} (last shell)	0.174 (0.196)	0.1733 (0.190)
R_{free} (last shell)	0.197 (0.206)	0.2203 (0.270)
RMS deviation bond lengths (Å)	0.008	0.008
RMS deviation bond angles (°)	0.94	0.92
Coordinate error (maximum likelihood estimate)	0.14 Å	0.22 Å
Total number of atoms	1867	1776
Protein residues	198	198
Protein	1587	1561
Ligand	88	49
Solvent	192	166
Mean B-factor	18.5	23.1
Protein	17.6	22.2
Ligand	13.4	24.2
Solvent	28.2	31.5
Ramachandran favored, allowed, outliers (%)	100, 0, 0	98.8, 1.0, 0

Table S2. Interaction Energies for Boronic Acid 1 and HIV-1 Protease Residue 30

HIV-1 Protease	Bond	ρ (eÅ^{-3})	$\nabla^2\rho$ (eÅ^{-5})	Bond Index
Wild-type	BO···H	0.270	–1.38	0.31
	BOH···OC	0.174	–0.08	0.22
D30N	BO···H	0.295	–1.68	0.32
	BOH···OC	0.172	0.03	0.20

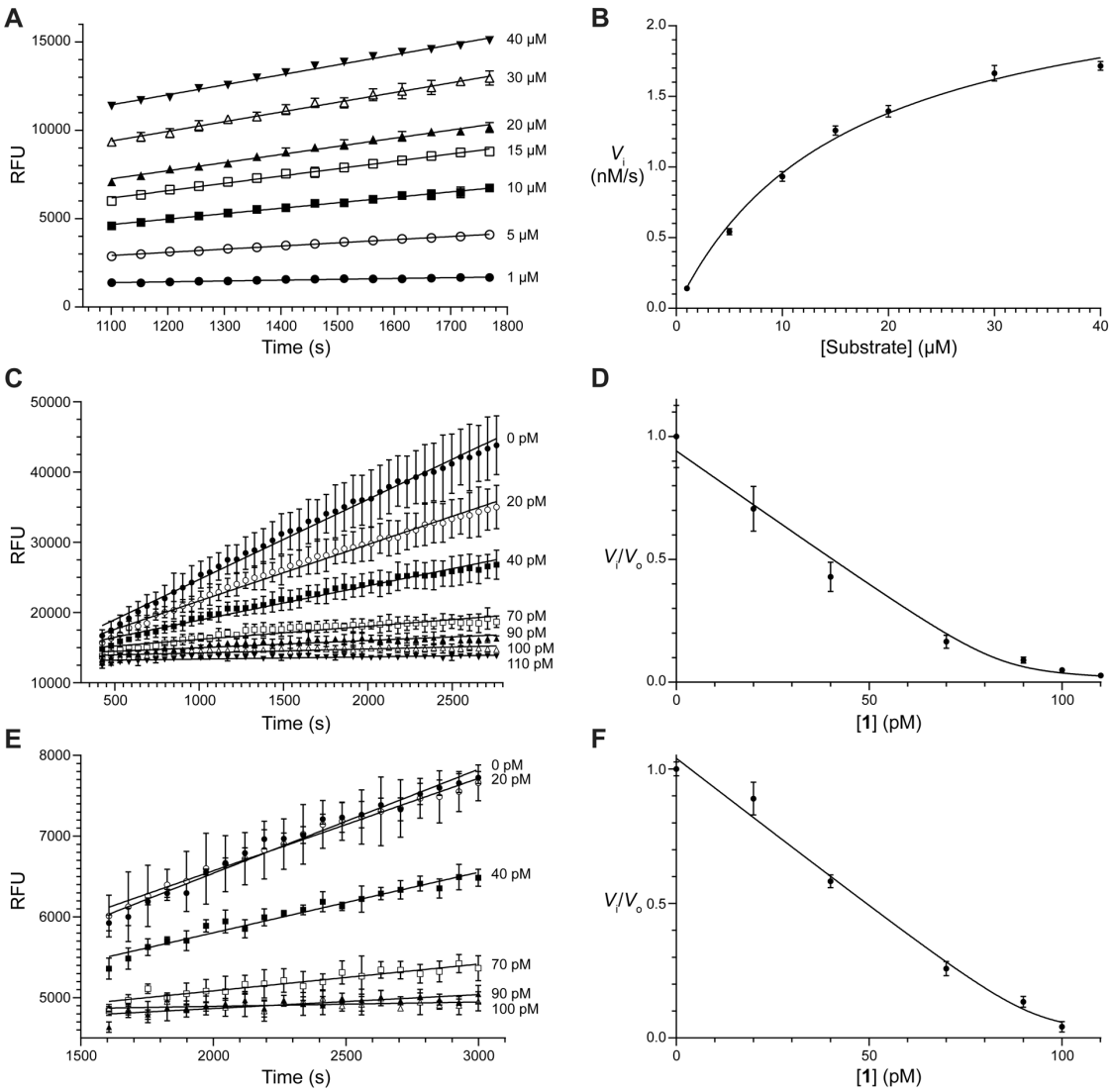

Figure S1. Raw and Processed Kinetic Data from Assays of HIV-1 Protease Activity. (A) Reaction progress curves of 5 nM D30N HIV-1 protease titrated with a fluorogenic substrate. (B) Non-linear fitting of reaction velocities to the Michaelis–Menten equation provides values of k_{cat} = 0.50 ± 0.01 s^{-1} and K_M = 16 ± 1 μM (R^2 = 0.99). (C) Reaction progress curves of 85 pM wild-type HIV-1 protease titrated with boronic acid **1** and 10 μM substrate. (D) Non-linear fitting of reaction velocities to Morrison's equation, providing a value of K_i = 0.5 ± 0.3 pM (R^2 = 0.96). (E) Reaction progress curves of 100 pM D30N HIV-1 protease titrated with boronic acid **1** and 10 μM substrate. (F) Non-linear fitting reaction velocities to Morrison's equation, providing a value of K_i = 0.4 ± 0.3 pM (R^2 = 0.98).

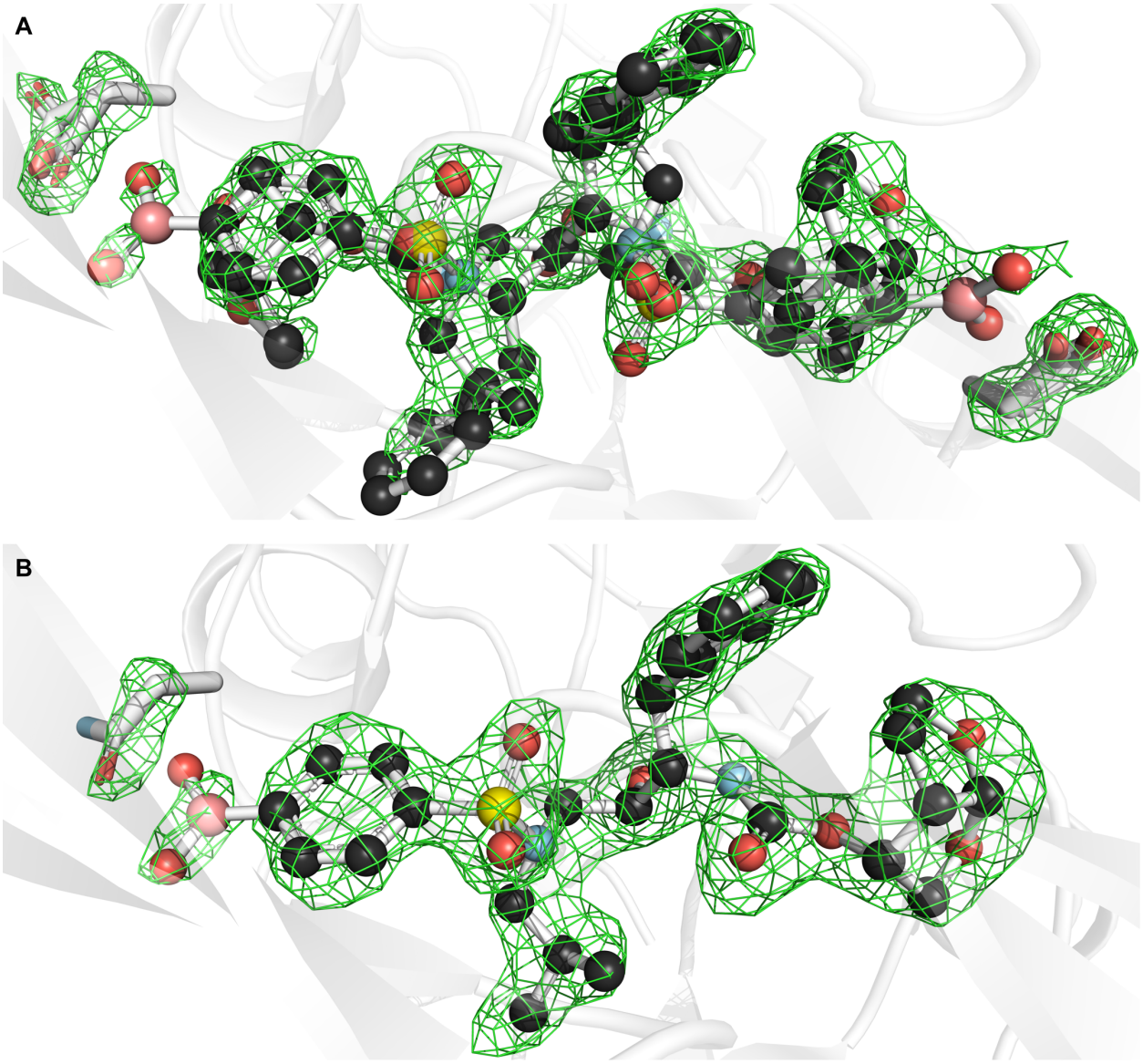

Figure S2. Depiction of electron density of HIV-1 proteases with bound boronic acid **1**. $F_o - F_c$ density maps resulting from simulated-annealing refinement with the ligand removed and residues proximal to the boronic acid replaced with glycine were overlayed on final models from (A) wild-type HIV-1 protease (PDB entry 6c8x) and (B) D30N HIV-1 protease (6c8y). Density is depicted at 3.0σ within 1.5 Å of side-chains proximal to boronic acid **1**.

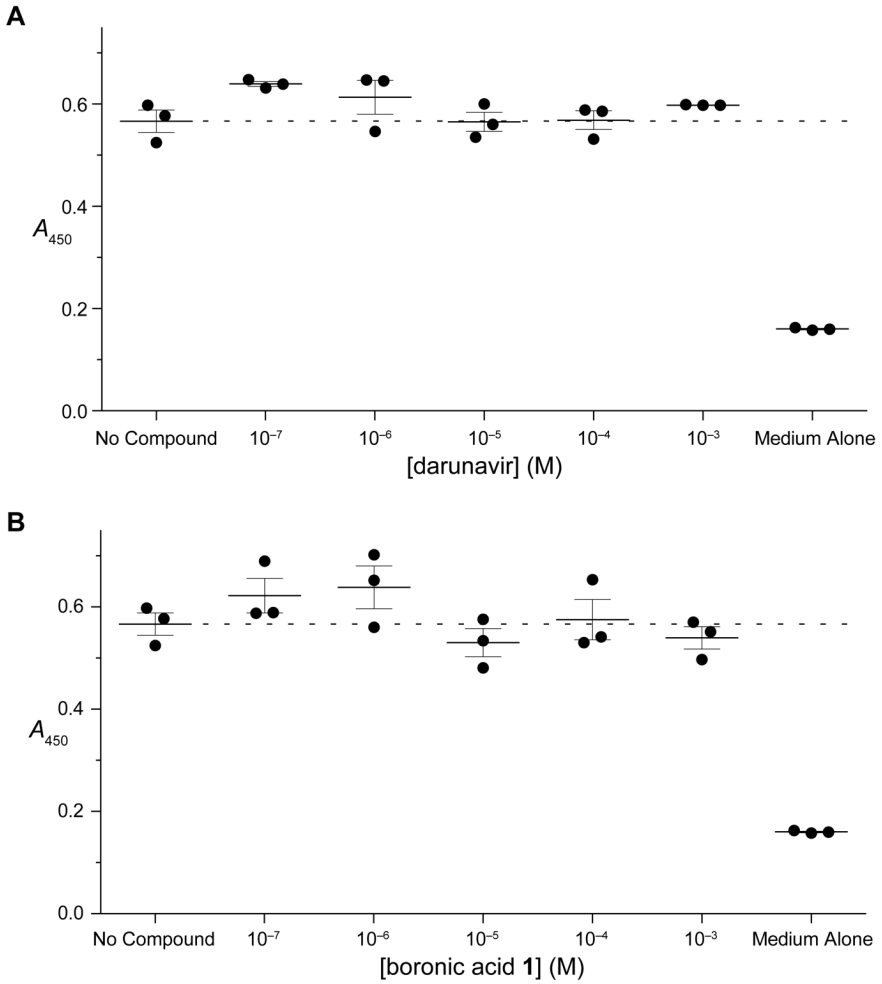

Figure S3. Toxicity of darunavir and boronic acid **1** for human cells. Graphs show the absorbance at 450 nm from a tetrazolium dye-based assay of the viability of MT-4 cells (adult T-cell leukemia) after incubation with darunavir (A) or boronic acid **1** (B) for 48 h. A high A_{450} value is indicative of viable cells.

NMR Spectra

^{1}H NMR Spectrum of Compound **S2** in $CDCl_3$

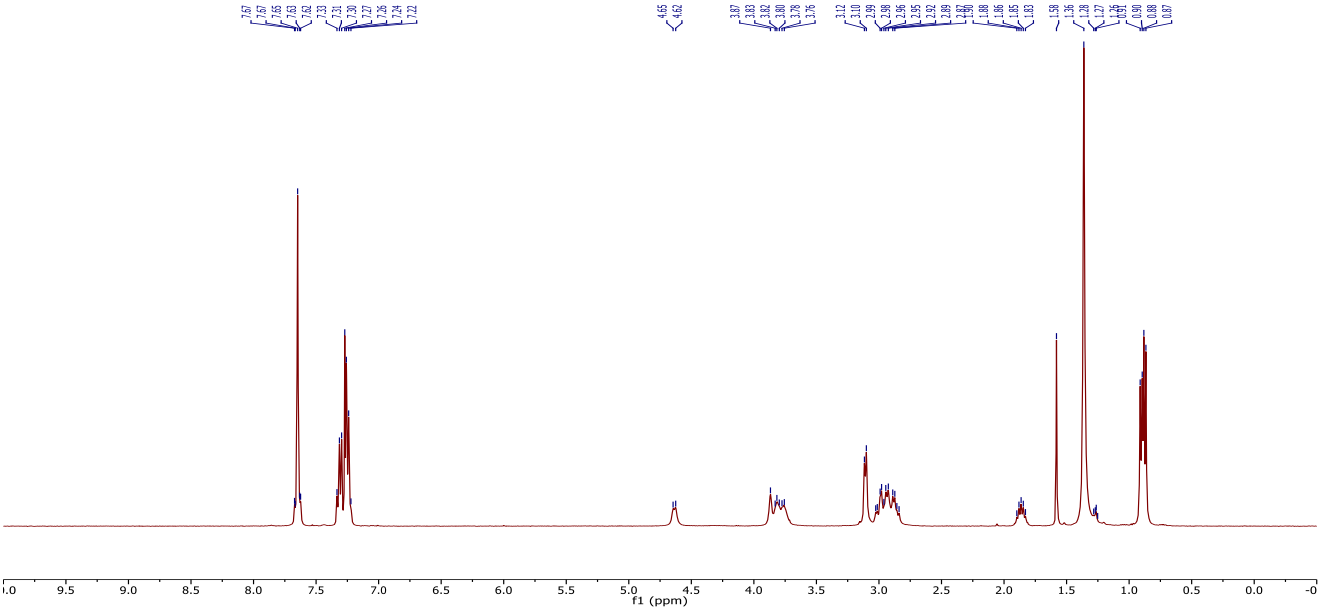

^{13}C NMR Spectrum of Compound **S2** in $CDCl_3$

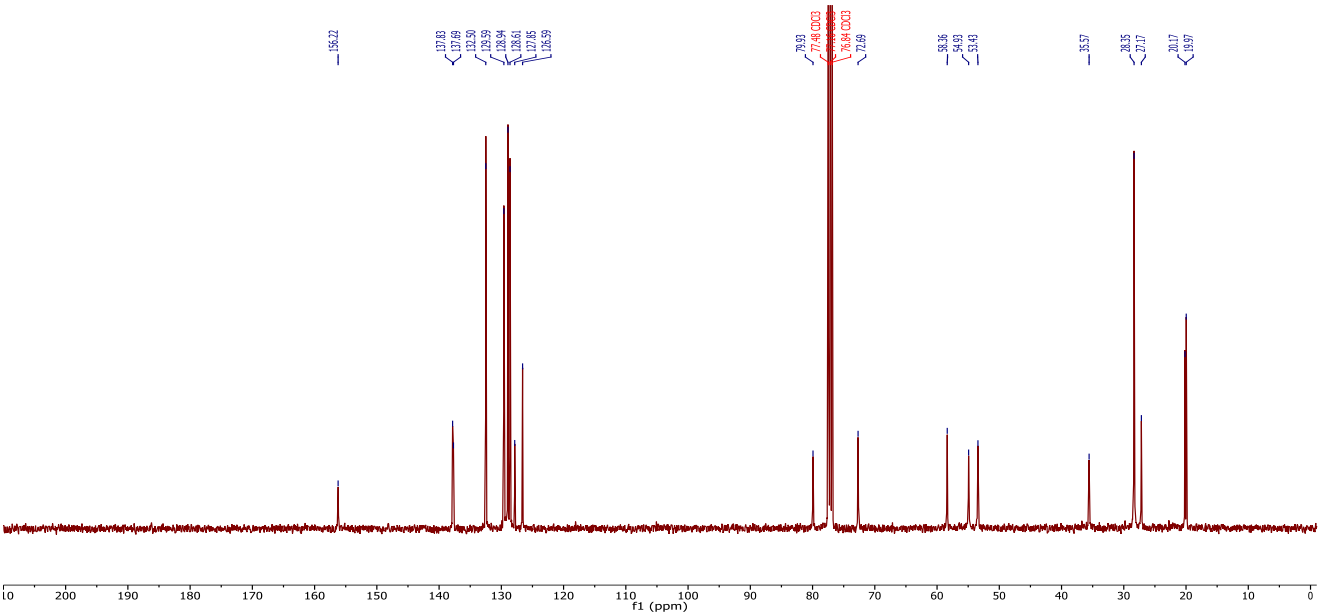

^{1}H NMR Spectrum of Compound **S3** in $CDCl_3$

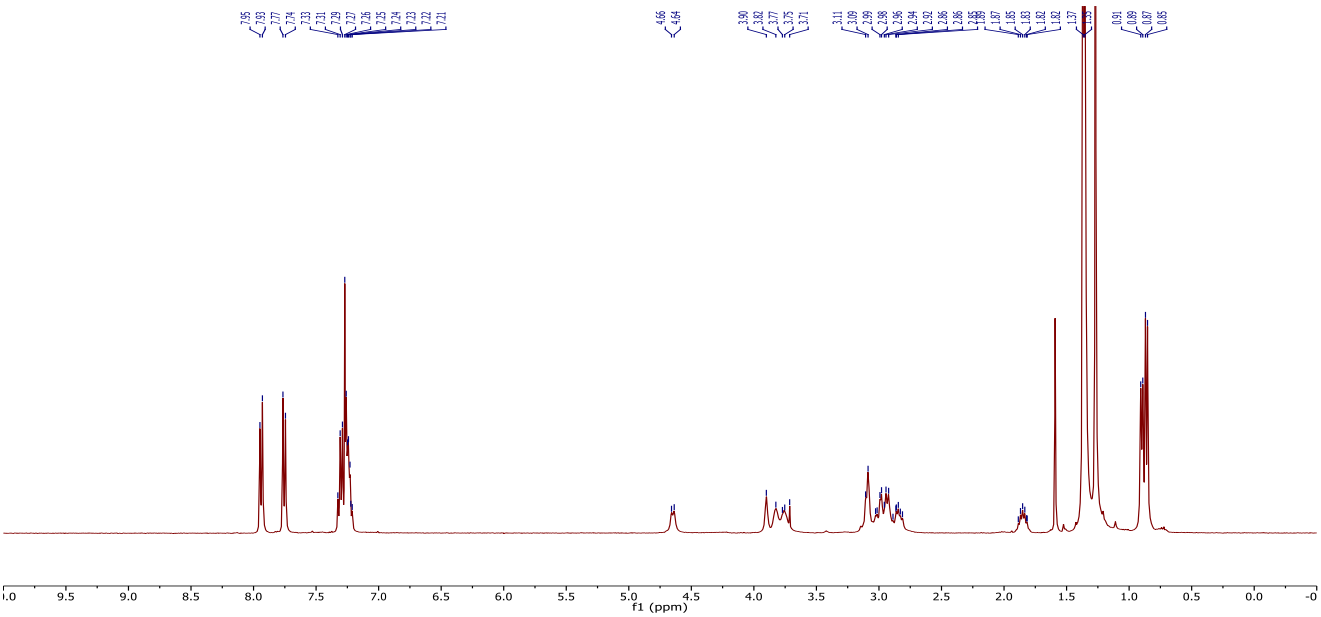

^{13}C NMR Spectrum of Compound **S3** in $CDCl_3$

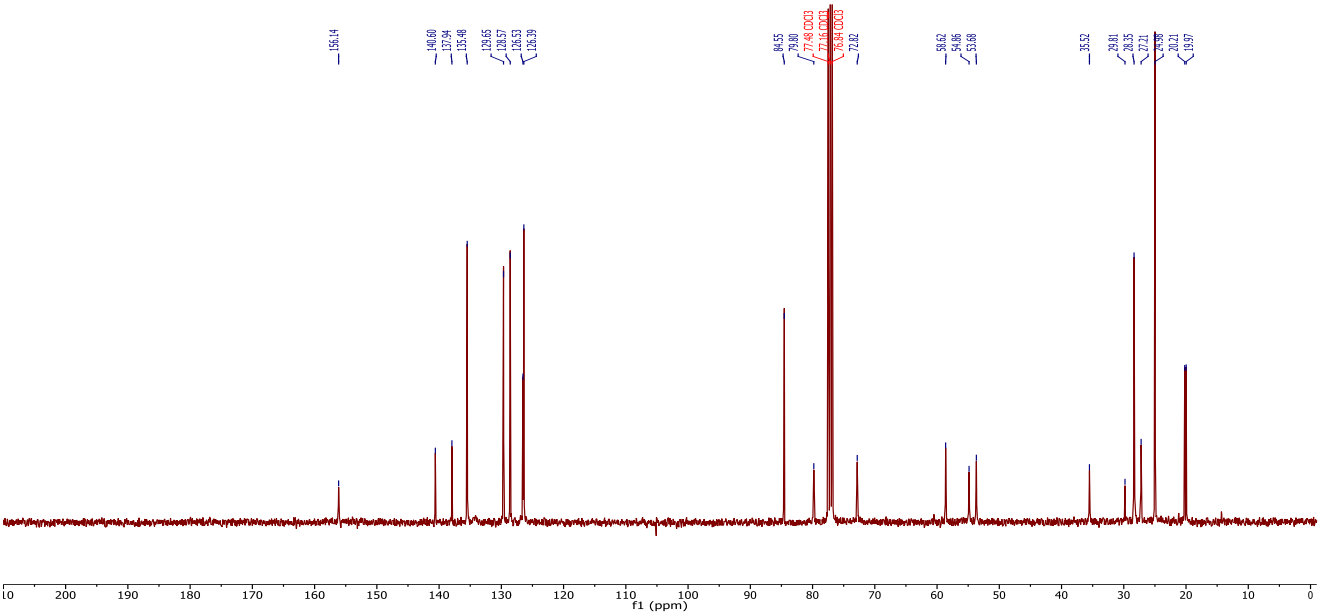

^{1}H NMR Spectrum of Compound **S5** in $CDCl_3$

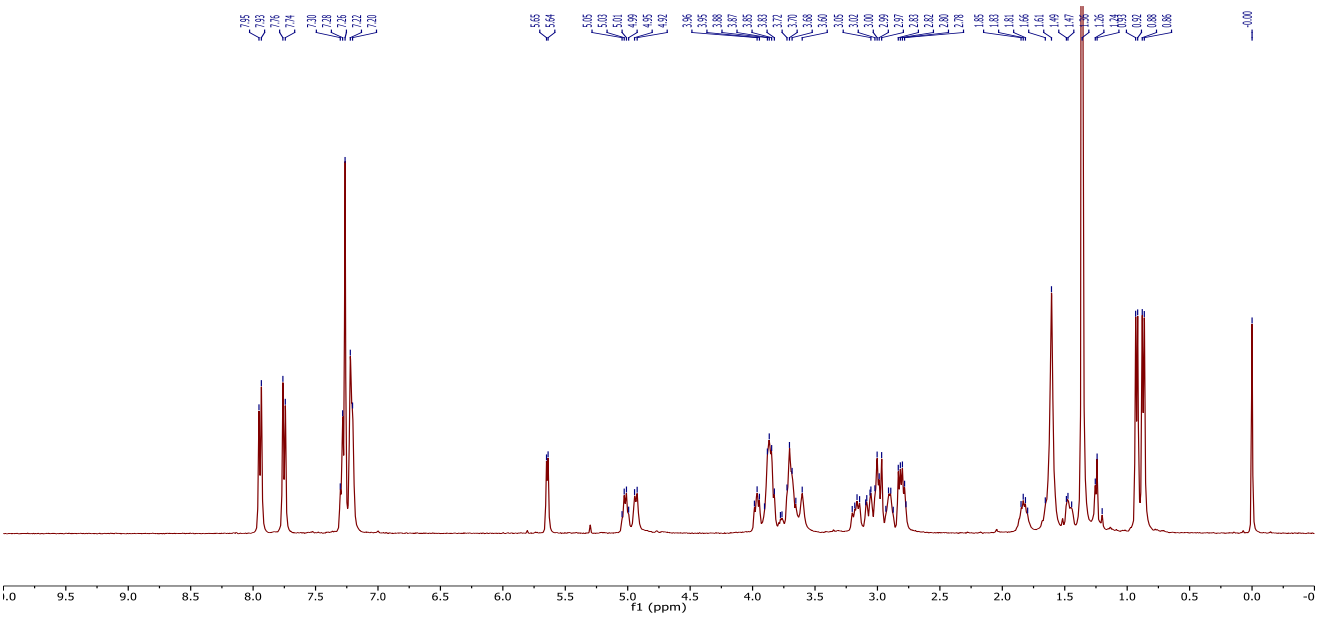

^{13}C NMR Spectrum of Compound **S5** in $CDCl_3$

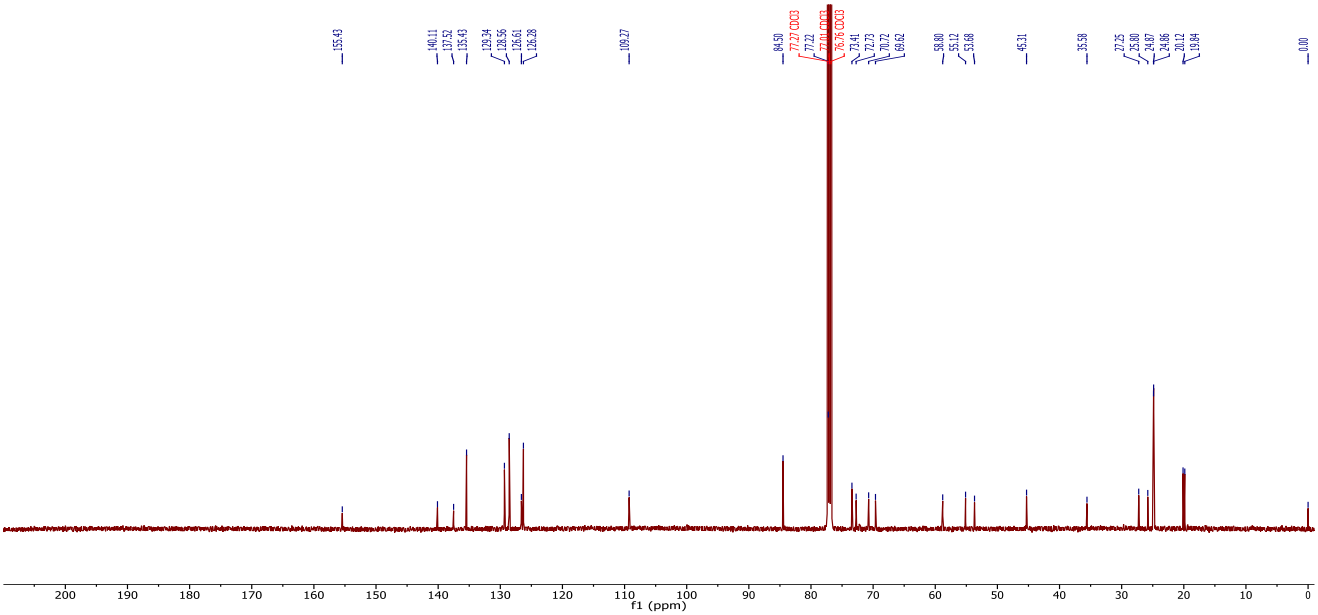

^{1}H NMR Spectrum of Compound **1** in Methanol-d_4

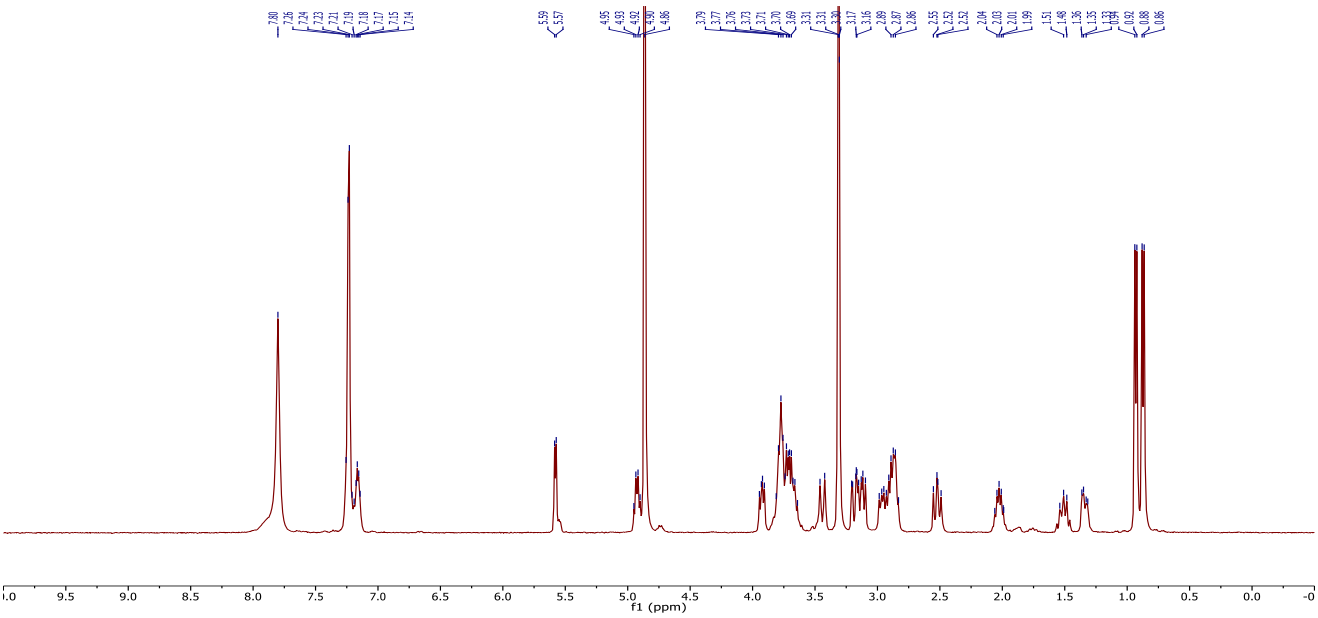

^{13}C NMR Spectrum of Compound **1** in Methanol-d_4